

# Solid-state compound phase formation of $\text{TiSi}_2$ thin films under stress

C. Theron<sup>a</sup>, N. Mokoena<sup>b,c</sup> and O.M. Ndwandwe<sup>b\*</sup>

Different stress situations were created on an Si(100) wafer by depositing either  $\text{Si}_3\text{N}_4$  or  $\text{SiO}_2$  thin films on the back side.  $\text{Si}_3\text{N}_4$  has a different thermal expansion coefficient from that of  $\text{SiO}_2$ . A thin Ti film was then deposited on the front side of the Si wafer. The structures were then annealed at various high temperatures for different periods of time. Real-time Rutherford backscattering spectrometry, as well as sample curvature measurements, were used to characterise the samples. Different reaction rates were found between  $\text{Si}_3\text{N}_4$ -deposited samples and  $\text{SiO}_2$ -deposited samples.

**Key words:** stress, thin films, real-time Rutherford backscattering spectrometry, phase formation,  $\text{TiSi}_2$ , diffusion

## Introduction

Stress is always present in thin films due to film deposition parameters. These parameters include the type of film that has been deposited, the rate of deposition, the method that was used to deposit the films, and the temperature of the substrate during deposition.<sup>1</sup> According to Yu,<sup>2</sup> stress in thin films may be divided into: thermal stress, due to the difference in thermal expansion coefficients of the film and the substrate; or intrinsic stress, which results from the growth and the structure of the films. For film thicknesses ( $t_f$ ) that are much smaller than substrate thicknesses ( $t_s$ ), Stoney's equation is generally used:<sup>1</sup>

$$\sigma_f = \frac{1}{6} \left( \frac{1}{R} - \frac{1}{R_o} \right) \frac{E_s t_s^2}{(1 - \nu_s) t_f}, \quad (1)$$

where  $E_s$  is Young's modulus,  $\nu_s$  is Poisson's ratio of the substrate, and  $R$  and  $R_o$  are the radii of curvature of the film before and after film deposition, respectively.

$\text{TiSi}_2$  is of great technological importance to the microelectronics industry and has widespread use in the fabrication of metal oxide semiconductor field effect transistors (MOSFET).<sup>3</sup>  $\text{TiSi}_2$  is a popular silicide because it has the lowest resistivity of all silicides.<sup>4,5</sup> This fact has resulted in many studies being done on the reaction between Ti and Si thin films.<sup>6</sup> Reports concerning first phase formation and phase formation sequence in the Ti-Si binary system vary. Some investigators have reported that  $\text{TiSi}_2$  is the only phase found at temperatures greater than 500°C.<sup>7</sup> Other studies show that all the Ti is converted to  $\text{TiSi}$ , before the formation of  $\text{TiSi}_2$ , at temperatures between 450°C and 700°C.<sup>8</sup>

Some investigators have performed rapid thermal annealing (RTA) studies and have found that  $\text{TiSi}$  first forms at temperatures between 450°C and 600°C.<sup>9</sup> There are however other investigators who reported  $\text{Ti}_5\text{Si}_4$  as a first phase during RTA studies.<sup>10</sup> In some investigations,  $\text{TiSi}$  grew simultaneously with  $\text{TiSi}_2$ ,  $\text{Ti}_5\text{Si}_4$  and  $\text{Ti}_5\text{Si}_3$ , at temperatures between 400°C and 600°C.<sup>11</sup>

<sup>a</sup>Department of Physics, University of Pretoria, Pretoria 0002, South Africa.

<sup>b</sup>Department of Physics and Engineering, University of Zululand, Private Bag X1001, KwaDlangezwa 3886, South Africa.

<sup>c</sup>Reactor Fuel Engineering Group, Koeberg Nuclear Power Station, Private Bag X10, Kernkrag 7440, South Africa.

\*Author for correspondence E-mail: muzi.ndwandwe@gmail.com

## Methods

Samples with the structures  $\text{SiO}_2/\text{Si}<100>$  or  $\text{Si}_3\text{N}_4/\text{Si}<100>$ , were chemically cleaned following a simple sequence. The following procedure was used: Samples were dipped, in sequence, in methanol, acetone, trichloroethylene, acetone and methanol, and then rinsed in ionised water. Finally, the samples were etched in a 20% solution of hydrofluoric acid to remove any native oxide layer that may be present. The role of the back side substrates,  $\text{SiO}_2$  and  $\text{Si}_3\text{N}_4$ , was to induce stress of different types during annealing. The samples were loaded in an ultra-high vacuum system where Ti of various thicknesses was deposited on the front side of the substrates. The vacuum during deposition was better than  $6 \times 10^{-7}$  torr. As a precaution, the samples were kept in a vacuum overnight to allow them to cool. Ti is known to easily oxidise in air, especially if its temperature is elevated. The resulting structures,  $\text{SiO}_2/\text{Si}<100>/\text{Ti}$  or  $\text{Si}_3\text{N}_4/\text{Si}<100>/\text{Ti}$ , were then annealed in a furnace at temperatures ranging from room temperature to 650°C. Ti was also deposited on  $\text{Si}<100>$  without a back side layer, under the same condition as the other samples.

In order to measure stress, sample thicknesses were accurately determined. First we used Rutherford backscattering spectrometry (RBS) in order to find layer thicknesses as well as to check whether the correct stoichiometry, in the case of back side  $\text{SiO}_2$  and  $\text{Si}_3\text{N}_4$ , had been obtained during sample preparation. A screw gauge was then used to determine wafer thickness.

## Results and discussion

Rutherford backscattering spectrometry results for the front side of the wafer showed that the thickness of the Ti was 550 Å. The thickness of the wafer, measured by means of a screw gauge, was found to be 6 230 000 Å.

From the relationship expressing change in length ( $\Delta L$ ) with change in temperature ( $\Delta T$ )

$$\alpha = \frac{\Delta L}{\Delta T}, \quad (2)$$

where  $L$  is the length of the film, we can express the ratio of the change in length of the film and the substrate in terms of expansion coefficients,

$$\frac{\Delta L_1}{\Delta L_2} = \frac{\alpha_1}{\alpha_2} \quad (3)$$

(since  $L_1 \approx L_2$ ). Results of such a calculation for the different sample categories in our experiment are summarised in Table 1. A ratio of less than one implies that a compressive stress will

**Table 1.** Thermal expansion coefficient ratios for different samples, based on Equations 2 and 3. A ratio less than 1 indicates compressive stress and a ratio greater than 1 indicates tensile stress.

Sample category	$\Delta L_1$ (deg) (silicon substrate)	$\Delta L_2$ (deg)	Elements and compounds	Ratios (see Eq. 2)
A	$1.4 \times 10^{-3}$	$2.5 \times 10^{-4}$	$\Delta L_{\text{Si}} / \Delta L_{\text{SiO}_2}$	5.60
B	$1.4 \times 10^{-3}$	$1.7 \times 10^{-3}$	$\Delta L_{\text{Si}} / \Delta L_{\text{Si}_3\text{N}_4}$	0.82
C	$1.4 \times 10^{-3}$	$4.3 \times 10^{-3}$	$\Delta L_{\text{Si}} / \Delta L_{\text{Ti}}$	0.33
D	$1.4 \times 10^{-3}$	$5.3 \times 10^{-3}$	$\Delta L_{\text{Si}} / \Delta L_{\text{TiSi}_2}$	0.27

**Table 2.** Calculated values of  $R_0$  (the sample radius before deposition of the front-side Ti film) and  $R_{\text{eff}}$  (the effective radius), and calculated values of stress for different categories of samples.

Category	$L$ (μm)	$b$ (Å)	$z = (1/2 t_s)$	$R_0$ (m)	$R_1$ (m)	$R_{\text{eff}}$ (m)	$\sigma_f$ (GPa)	$\sigma_s$ (MPa)
A	3 399	-512.5	$311.5 \times 10^{-6}$	-40.34	-28.21	-93.8	-2.8	-0.74
B	4 481	3 201.5	$311.5 \times 10^{-6}$	11.47	7.84	24.8	10.5	2.79
C	4 828	4 171.5	$311.5 \times 10^{-6}$	8.022	6.98	53.8	4.9	1.29

develop on the front side of the sample upon heating (a ratio bigger than one implies a tensile stress will develop).

Equation 4<sup>10</sup> was used to calculate the stress in the deposited film:

$$\sigma_f = \left( \frac{E_s}{1 - \nu_s} \right) \frac{d_s^2}{6d_f} \frac{8\Delta b}{L^2} , \quad (4)$$

where

$$\frac{8\Delta b}{L^2} = \frac{1}{r_{\text{eff}}} = \left( \frac{R_0 - R_1}{RR_0} \right) , \quad (5)$$

and  $\Delta b = b - b_0$ , thus the bow is related to the experimental radius ( $R_1$ ),  $b$  is its value after deposition and  $b_0$  the value before deposition (Fig. 1).

$$R = \frac{L^2}{8b} . \quad (6)$$

The stress is calculated on the entire sample since it has a depth of focus in the substrate ( $\sigma_{si}(z)$ ). The stress depth is calculated using the following equation:

$$\sigma_{si}(z) = \left( \frac{E_s}{1 - \nu_s} \right) \frac{z}{r_{\text{eff}}} , \quad (7)$$

where  $z = 0$  in the middle of the substrate and  $z = [1/2(623)] = 311.5$  at the front side deposited with Ti.

Stress was calculated using Stoney's equation, as given by Equation 1, and the value of  $R_1$  was determined from Equation 6. Radius measurements were obtained using a profilometer. This gave the length ( $L$ ) and bow value ( $b$ ) that was used to calculate radius  $R_1$ . After the calculation of the sample radius ( $R_1$ ),  $R_0$ , the original radius before deposition of Ti, was obtained by using the radius effect.<sup>10</sup> The two values,  $R_1$  and  $R_0$ , were then used to find the effective radius ( $R_{\text{eff}}$ ) of each sample.  $R_{\text{eff}}$  allowed us to calculate the stress after deposition. Table 2 summarises the results of the calculation.

The negative sign on stress values indicate that the stress is compressive, while positive values indicate tensile stress. The stress is induced in the thin film when deposition takes place on the bare substrate. The sample heats up slightly during deposition and then cools after deposition is completed. When the film is being deposited on top of the substrate in a vacuum, by means of electron beam evaporation, it heats up due to the flux of energetic particles landing on the substrate and also because radiative heat is released from the molten material being deposited from the crucible. The composite film now has multilayers, which on cooling contract by unequal amounts due to different expansion coefficients of the different films. Thermal expansion coefficients of metallic films are generally larger in value when compared to those of silicon. But  $\text{SiO}_2$  has an even smaller expansion coefficient compared to that of Si.  $\text{Si}_3\text{N}_4$  has a larger expansion coefficient compared to Si (Fig. 2 and Table 3).

The front side film is therefore deposited at a temperature which is higher than room temperature because of the

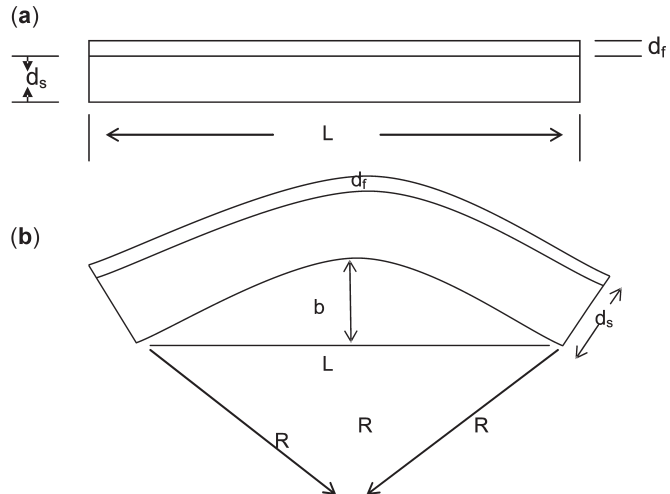


**Fig. 1.** This diagram shows how the different variables referred to in the text have been defined. Sample thickness is  $d_s$ , front side film thickness is  $d_f$ ,  $b$  is the bow parameter,  $L$  is the length of the sample and  $R$  is the curvature of the sample.

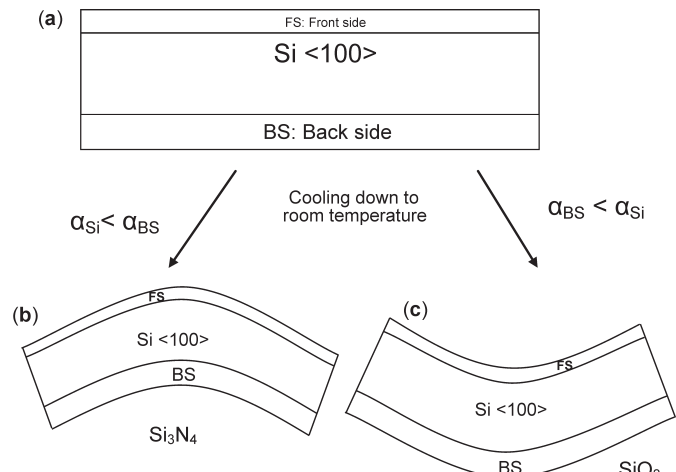


**Fig. 2.** A diagram showing that the sample BS/Si<100>/Ti bends when it cools, if the layers have different expansion coefficients ( $\alpha$ ). For a back side layer consisting of  $\text{Si}_3\text{N}_4$  (whose expansion coefficient is higher than that of Si), the front side (and hence the Ti layer) will be subjected to a tensile stress. The opposite will happen for a sample having  $\text{SiO}_2$  on its back side ( $\alpha_{\text{SiO}_2} < \alpha_{\text{Si}}$ ).

**Table 3.** Thermal expansion coefficients ( $\alpha$ ) for Ti,  $\text{SiO}_2$ ,  $\text{Si}_3\text{N}_4$  and  $\text{TiSi}_2$ . The Table also gives the values used previously and those selected for use in this study.

$\text{TiSi}_2$	Thermal expansion coefficients ( $\alpha$ ) $\times 10^6 \text{ K}^{-1}$				
	Ti	$\text{SiO}_2$	Si	$\text{Si}_3\text{N}_4$	Reference
-	-	0.5	3	2.5	4
-	8.6	-	2.8	-	5
-	-	-	-	3.4	6
-	-	0.5	-	-	7
-	-	-	-	3.3	8
10.5	-	-	-	-	9
10.5	8.6	0.5	2.8	3.35	Used in this study

unintended heating effects explained before. When the sample cools down, the layer that has a higher expansion coefficient shrinks to a greater extent, causing either compressive stress or tensile stress on the front surface. In the case of a sample with structure  $\text{SiO}_2/\text{Si}/\text{Ti}$ —if one neglects the effect of the Ti, since it is much thinner than the other two films— $\text{SiO}_2$  will shrink less than Si, causing the front surface, and hence the Ti film, to be under compressive stress at room temperature.  $\text{Si}_3\text{N}_4$  has a thermal expansion coefficient greater than that of Si. On cooling,  $\text{Si}_3\text{N}_4$  will contract more than Si, leading to a tensile stress in the front of the film, where Ti is located (Fig. 2).

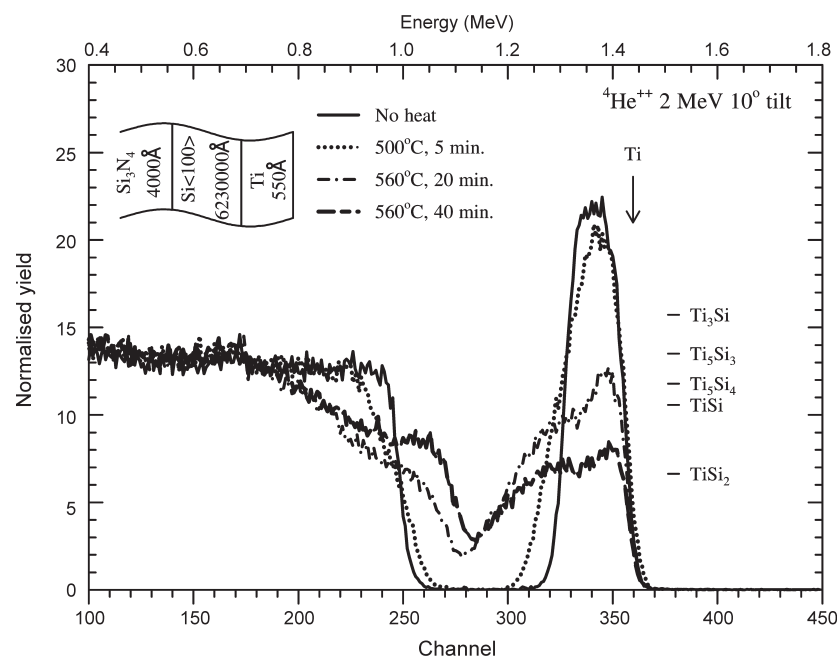
#### Normal Rutherford backscattering spectrometry

Figure 3 shows Rutherford backscattering spectra of a multilayered film made up of a  $\text{Si}<100>$  wafer onto which  $4\,000\text{ \AA}$  of  $\text{Si}_3\text{N}_4$  was deposited on the back side. The wafer itself is  $6\,230\,000\text{ \AA}$  thick. On the front side of the wafer,  $550\text{ \AA}$  of Ti was deposited. Rutherford backscattering spectrometry results showed no observable reaction for samples annealed at temperatures below  $500^\circ\text{C}$  (not shown here). The spectrum of the sample annealed at  $500^\circ\text{C}$  for 5 min showed interdiffusion between Ti and Si. This is indicated by the change in the gradient on the edge of the spectrum of Ti (that is in contact with Si), which changed from steep to less steep. No shoulder developed, indicating that no reaction took place. The spectrum of the sample annealed at  $560^\circ\text{C}$  for 20 min has a shoulder corresponding to the formation of  $\text{TiSi}$ . The formation of  $\text{TiSi}$  as a first phase in the Ti-Si thin films binary system has been observed previously by others.<sup>8</sup> The presence of a compressive stress (at high temperature) on the front side of the wafer, due to  $\text{Si}_3\text{N}_4$  on its back side, has therefore not led to any change in first phase formation for this binary system. The spectrum of the sample annealed at  $560^\circ\text{C}$  for 40 min showed the presence of  $\text{TiSi}_2$  (Fig. 3).

Samples comprised of  $\text{SiO}_2(4\,000\text{ \AA})/\text{Si}<100>(5\,300\text{ \AA})/\text{Ti}(550\text{ \AA})$  were annealed at various temperatures. Figure 4 shows the spectra of a virgin sample and a sample annealed at  $590^\circ\text{C}$  for 40 min; it can be observed that  $\text{TiSi}$  formed on the annealed sample. Rutherford Universal Manipulation Program simulation showed that there was still Ti remaining on this sample after annealing. The sample was, however, already in an advanced state of reaction. It was not possible from the results obtained to determine at what exact temperature the reaction started on the samples with  $\text{SiO}_2$  on their back side. To solve this problem, we performed *in situ* real-time RBS.

#### *In situ* real-time Rutherford backscattering spectrometry

In order to observe when the reaction starts and how it proceeds with time, *in situ* annealing and spectrum collection from RBS were done simultaneously in a chamber whose vacuum was better than  $10^{-6}$  torr. The heating was done by ramping the tem-



**Fig. 3.** Rutherford backscattering spectra of  $\text{Si}_3\text{N}_4(4\,000\text{ \AA})/\text{Si}<100>(6\,230\,000\text{ \AA})/\text{Ti}(550\text{ \AA})$  samples, deposited and annealed at various temperatures. The spectrum of the sample annealed at  $500^\circ\text{C}$  for 5 min showed no reaction, but showed interdiffusion between Si and Ti. Annealing at  $560^\circ\text{C}$  for 20 min led to the formation of  $\text{TiSi}$ , and annealing for 40 min resulted in the formation of  $\text{TiSi}_2$ .

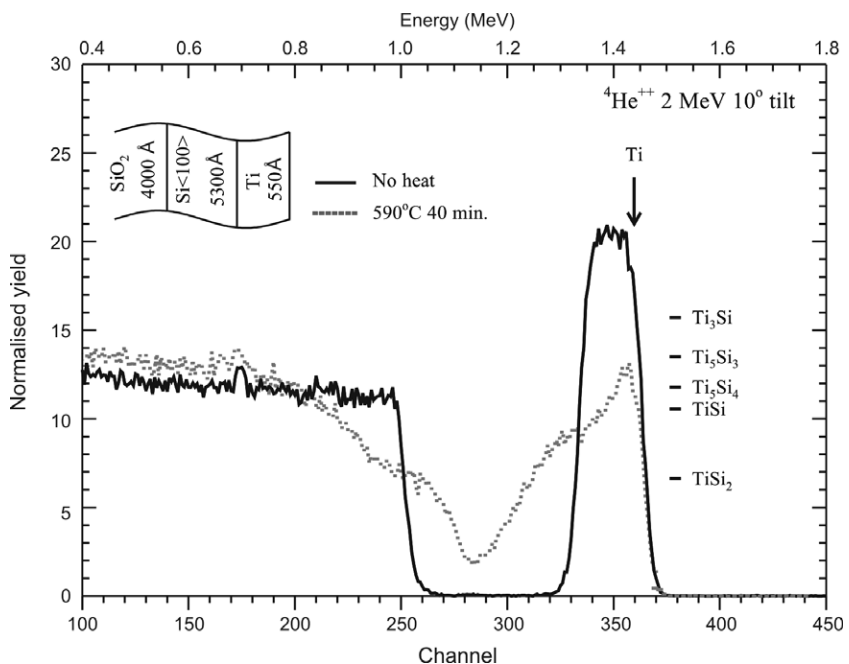


**Fig. 4.** Rutherford backscattering spectra of samples with  $\text{SiO}_2$  on the back side. It was determined that the  $\text{SiO}_2$  layer on the back side was  $4\,000\text{ \AA}$  thick (spectrum not shown here). The spectrum of the virgin sample showed that the Ti layer on the front side was  $550\text{ \AA}$  thick. The spectrum of the sample annealed at  $590^\circ\text{C}$  for 40 min showed that  $\text{TiSi}$  had formed.

perature, at a rate of  $20^\circ\text{C min}^{-1}$ , from room temperature ( $\sim 20^\circ\text{C}$ ) to  $340^\circ\text{C}$ . Thereafter, it was ramped at a rate of  $3^\circ\text{C min}^{-1}$  and allowed to rise to a value of  $650^\circ\text{C}$ . Figure 5a shows the temperature versus time curve as measured on the sample. Figures 5b and 5c show a three-dimensional view of the spectrum from a sample of a  $6\,230\,000\text{ \AA}$  thick  $\text{Si}<100>$  wafer with  $4\,000\text{ \AA}$  of  $\text{SiO}_2$  deposited on the back side and  $550\text{ \AA}$  Ti on the front side. Figure 5b shows that there is no observable reaction between Si and Ti during the time period from 0 min to about 80 min (which corresponds to a temperature of about  $500^\circ\text{C}$ ). A more in depth analysis of the spectra that make up Fig. 5 showed that  $\text{TiSi}$

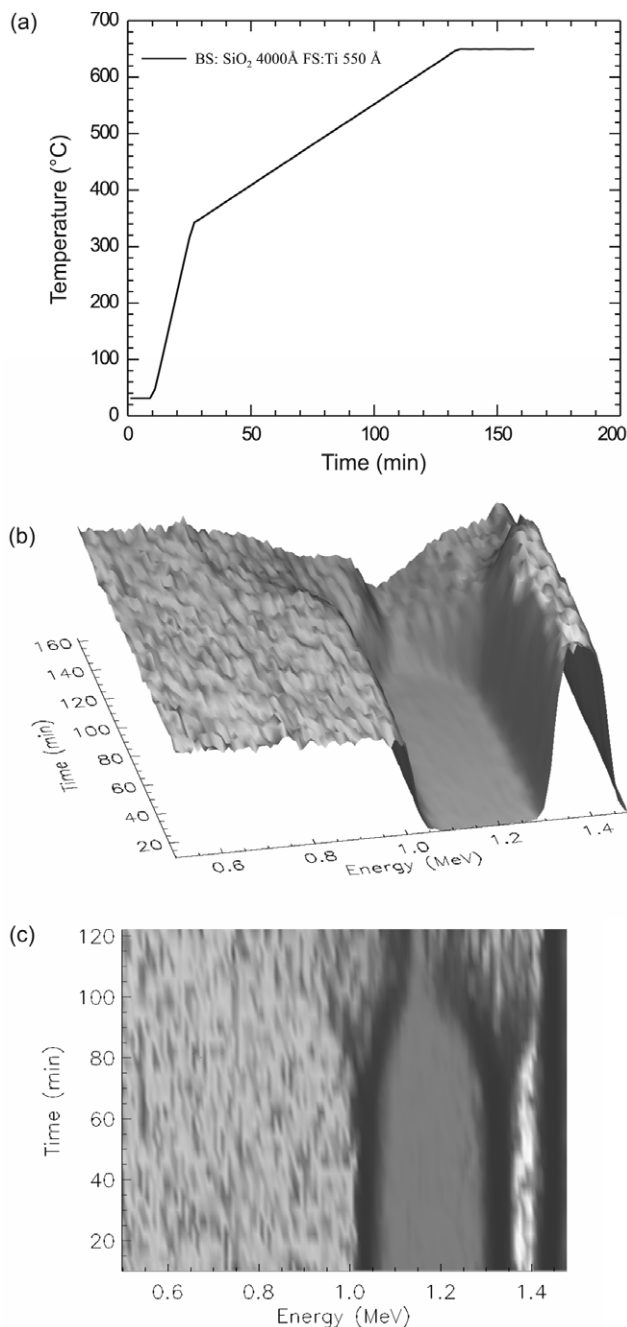


**Fig. 5.** (a) The temperature versus time profile of a sample of 6 230 000 Å thick Si<100> wafer with 4 000 Å of SiO<sub>2</sub> on the back side and 550 Å Ti on the front side. (b) A three-dimensional view of the spectrum of the same sample. Time and energy are plotted on the horizontal axes and counts on the vertical axis. (c) Above view of the spectrum in (b).

began forming at that stage. It continued growing until about 110 min after starting the ramp. This time corresponds to a temperature of about 580°C. At that stage, TiSi<sub>2</sub> formation was observed. These observations are in line with what was observed using normal RBS.

Annealing of the sample with Si<sub>3</sub>N<sub>4</sub> on the back side was done by ramping the temperature, at a rate of 20°C min<sup>-1</sup>, from room temperature (~20°C) to 440°C. It was thereafter ramped at 3°C min<sup>-1</sup>, to 650°C. Rutherford backscattering spectrometry analysis on the sample with Si<sub>3</sub>N<sub>4</sub>, with a structure of Si<sub>3</sub>N<sub>4</sub>(400 Å)/Si(6 230 000 Å)Ti(400 Å), showed that the reaction for the formation of TiSi started at about 570°C, and formation of TiSi<sub>2</sub> started at about 610°C. Both phases (TiSi and TiSi<sub>2</sub>) grew simultaneously thereafter with increasing temperature (RBS results not shown).

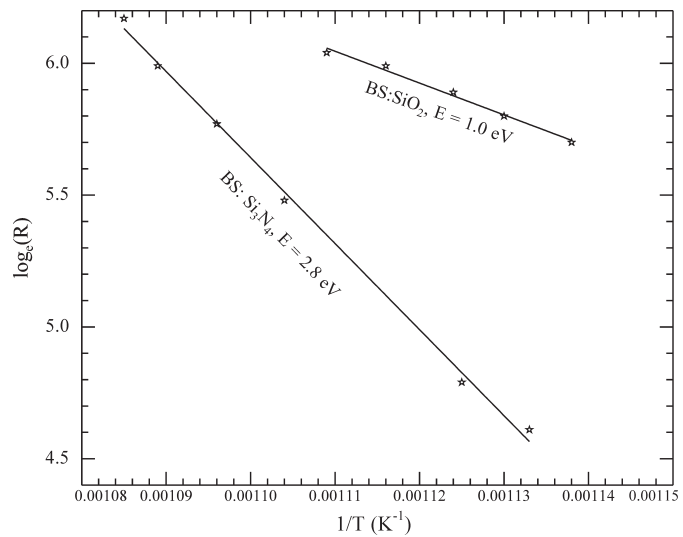


**Fig. 6.** An Arrhenius plot for the growth of TiSi<sub>2</sub> for samples with SiO<sub>2</sub> deposited on the back side and for samples with Si<sub>3</sub>N<sub>4</sub> deposited on the back side. The activation energies for the growth of TiSi<sub>2</sub> were 1.0 ± 0.064 eV and 2.8 ± 0.076 eV, respectively.

**Table 4.** Sample thicknesses determined by Rutherford backscattering spectrometry and screw gauge measurements.

Sample category	Back side layer	Substrate	Front side layer
A	SiO <sub>2</sub> (4000 Å)	Si(100) 6.23 × 10 <sup>6</sup> Å	Ti (550 Å)
B	Si <sub>3</sub> N <sub>4</sub> (4000 Å)	Si(100) 6.23 × 10 <sup>6</sup> Å	Ti (550 Å)
C	Si <sub>3</sub> N <sub>4</sub> (2000 Å)	Si(100) 6.23 × 10 <sup>6</sup> Å	Ti (550 Å)

The RUMP simulation program was used to analyse the thicknesses of grown phases at different temperatures. Table 4 summarises the values of sample thicknesses observed.

Figure 6 is an Arrhenius plot for the growth of the phase TiSi<sub>2</sub>, for the samples with SiO<sub>2</sub> deposited on the back side and with Si<sub>3</sub>N<sub>4</sub> deposited on the back side. The activation energy for the growth of TiSi<sub>2</sub> in which the back side film was SiO<sub>2</sub> was 1.0 ± 0.064 eV, and the activation energy for the growth of TiSi<sub>2</sub> in which the back side film was Si<sub>3</sub>N<sub>4</sub> was 2.8 ± 0.076 eV.

### Conclusion

We investigated the interfacial reaction between Si and Ti by depositing either SiO<sub>2</sub> or Si<sub>3</sub>N<sub>4</sub> on the back side of a Si<100> wafer, so as to induce stress on the front side. Such stresses could be either compressive or tensile. A layer of Ti, which was much thinner than either the substrate Si or the back side layer, was then deposited on the front side of the wafer.

Characterisation of the samples, using RBS, after annealing in a vacuum at high temperatures revealed that TiSi formed first, followed by TiSi<sub>2</sub>. *In situ* real-time RBS allowed us to follow the process step-by-step and to more accurately determine the starting temperatures for phase formation. Real-time RBS showed that, for a sample with SiO<sub>2</sub> on its back side, formation of TiSi started at 500°C, while TiSi<sub>2</sub> began to form at 580°C. In the case of the sample with Si<sub>3</sub>N<sub>4</sub>, TiSi began forming at 570°C and TiSi<sub>2</sub> at 610°C.

Activation energy for the formation of TiSi<sub>2</sub> on the sample with a back side layer of SiO<sub>2</sub>, was found to be 1.0 ± 0.064 eV, while that for a sample with a back side layer of Si<sub>3</sub>N<sub>4</sub>, was found to be 2.8 ± 0.076 eV. Values of stress calculated at room temperature for a sample with SiO<sub>2</sub> on its back side was found to be -2.8 GPa, while for a sample with Si<sub>3</sub>N<sub>4</sub>, it was 10.5 GPa.

It must be noted that in this experiment the annealing temper-

atures ( $>400^{\circ}\text{C}$ ) were much higher than the deposition temperatures ( $<100^{\circ}\text{C}$ ), which in turn were higher than the temperatures at which stress measurements were made. It was found that the sample with  $\text{SiO}_2$  on its back side displayed compressive stress on its front side at room temperature. When such a sample is annealed, the temperature-induced stress should reduce, reach a minimum at its deposition temperature and then rise again (but with an opposite sign) above the deposition temperature. This sample should therefore display tensile stress on its front side at the temperature at which phases form. Tensile stress causes the appearance of vacancies on the front side, thus leading to an easier diffusion of atoms (and hence a lower activation energy). The opposite should happen for a sample with  $\text{Si}_3\text{N}_4$  on its back side.

Received 23 October 2008. Accepted 25 August 2009.

1. Mayer J.W. and Lau S.S. (1990). *Electronic Materials Science: for Integrated Circuits in Si and GaAs*. Macmillan, New York.

2. Yu J.S., Mariaty A.M. and Knorr D.B. (1997). Model for predicting thermal stresses in thin polycrystalline films. *J. Mech. Phys. Solids* **45**, 511–534.
3. La Via F., Privitera S., Grimaldi M.G., Rimini E., Quilici S. and Meinardi F. (2000). Determination of C54 nucleation site density in narrow stripes by sheet resistance measurements and  $\mu$ -Raman spectroscopy. *Microelectron. Eng.* **50**, 139.
4. Nicolet M.A. and Lau S.S. (1983). *VLSI Electronics Microstructure Science*, ed. N. Einspruck, p. 415. Academic Press, New York.
5. Grovenor C.R.M. (1989). *Microelectronics Materials*, p. 68. Adam Hilger, Bristol and Philadelphia.
6. Pretorius R., Theron C.C. and Marais T.K. (1993). Evaluation of anomalies during nickel and titanium silicide formation using the effective heat of formation model. *Mater. Chem. Phys.* **36**, 31.
7. Beyers R. and Sinclair R. (1985). Metastable phase formation in titanium-silicon thin films. *J. Appl. Phys.* **57**, 5240.
8. Pico C.A. and Legally M.G. (1988). Kinetics of titanium silicide formation on single crystal Si: Experiment and modeling. *J. Appl. Phys.* **64**, 4957.
9. Wei C.S., van der Spiegel J. and Santiago J. (1985). Electrical characteristics of fast radiatively processed titanium silicide thin films. *J. Vac. Sci. Technol. A* **3**, 2259.
10. Dexin C.X., Harrison H.B. and Reeves G.K. (1988). Titanium silicide formed by rapid thermal vacuum processing. *J. Appl. Phys.* **63**, 2171.
11. Lakshmikumar S.T. and Rastogi A.C. (1989). The growth of titanium silicides in thin film Ti/Si structures. *J. Vac. Technol. B* **7**, 604.